

Long non-coding RNA FAM83A antisense RNA 1 (lncRNA FAM83A-AS1) targets microRNA-141-3p to regulate lung adenocarcinoma cell proliferation, migration, invasion, and epithelial-mesenchymal transition progression

Hongyu Huang^{a, #}, Chuyi Yang^{a, #}, Qichen Zhang^b, Ting Zhuo^a, Xiaohong Li^a, Nijiao Li^a, Lu Zhu^a, Chenyang Luo^a, Jinyan Gan^a, and Yanbin Wu^a

^aDepartment of Pulmonary and Critical Care Medicine, The First Affiliated Hospital of Guangxi Medical University, Nanning, China;

^bDepartment of the Bone and Joint Surgery, The First Affiliated Hospital of Guangxi Medical University, Nanning, China

ABSTRACT

The current paper investigates how long non-coding RNA (lncRNA) FAM83A antisense RNA 1 (lncRNA FAM83A-AS1) affected the epithelial-mesenchymal transformation (EMT), growth, invasion and migration of lung adenocarcinoma (LUAD) via targeting miRNA-141-3p. The GEPIA and ENCORI databases were used to analyze differences in lncRNA FAM83A-AS1 levels within LUAD samples. FAM83A-AS1 and miR-141-3p levels were assessed using qRT-PCR among 30 LUAD samples and surrounding normal tissues. In addition, we analyzed how FAM83A-AS1 affected proliferation, invasion, migration, and EMT processes of LUAD cells by targeting miR-141-3p through EdU, CCK-8 assay, scratch assay, transwell migration and invasion assay, immunofluorescence (IF) staining and WB assay. MicroRNAs targeting FAM83A-AS1 were screened using AnnoLnc2 and identified by RT-qPCR. Dual-luciferase assays were utilized to evaluate the connection between FAM83A-AS1 and miR-141-3p. FAM83A-AS1 expression was remarkably raised in lung cancer cells and tissue samples; however, miR-141-3p level markedly reduced relative to healthy samples. FAM83A-AS1 silencing suppressed EMT, growth, invasion and migration of LUAD cells. MiR-141-3p was the possible FAM83A-AS1 binding target negatively associated with FAM83A-AS1. The miR-141-3p inhibitor partly abolished the FAM83A-AS1 knockdown-induced inhibition on EMT, cell growth, invasion and migration in LUAD cells. In addition, miR-141-3p down-regulation abolished the inhibition of E-box-bound zinc finger protein 1 and 2 protein production following FAM83A-AS1 knockdown. According to our results, FAM83A-AS1/miR-141-3p axis plays an important role in LUAD occurrence and development. FAM83A-AS1 sponged miR-141-3p to down-regulate the level of the latter within LUAD and thereby encouraging LUAD development and suggesting a possible novel therapeutic approach for LUAD.

ARTICLE HISTORY

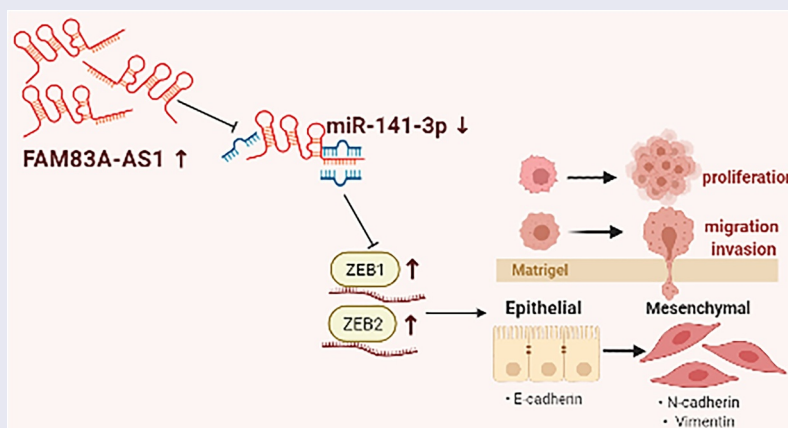
Received 4 December 2021



Revised 29 January 2022

Accepted 31 January 2022

KEYWORDS

FAM83A-AS1; lung adenocarcinoma; miR-141-3p; EMT; long non-coding RNAs



CONTACT Yanbin Wu  yanbin_w2021@126.com  Department of Pulmonary and Critical Care Medicine, The First Affiliated Hospital of Guangxi Medical University, Nanning, China

#These authors contributed equally to this work

© 2022 The Author(s). Published by Informa UK Limited, trading as Taylor & Francis Group.

This is an Open Access article distributed under the terms of the Creative Commons Attribution-NonCommercial License (<http://creativecommons.org/licenses/by-nc/4.0/>), which permits unrestricted non-commercial use, distribution, and reproduction in any medium, provided the original work is properly cited.

Cancer is a massive health problem affecting individuals worldwide, and it accounts for a major factor leading to mortality in USA. In 2021, cancer incidence in the United States was approximately 12%, with a mortality rate of 22% [1]. Non-small-cell lung cancer (NSCLC) and small-cell lung cancer (SCLC) stand for 2 lung cancer (LC) subtypes, among which, the former occupies about 85% of LC patients [2,3]. Despite early diagnosis and considerable breakthroughs in diagnosing and treating LUAD, mortality in advanced patients remains relatively high, and poor prognosis [4,5]. As a result, the specific molecular mechanisms of LUAD development must be discovered to uncover novel biomarkers which might be used to identify new targets for successful intervention, critical for early detection, prevention, and therapy.

Non-coding RNAs (ncRNAs) occupy around 98% of the whole human transcriptome, among which, long non-coding RNAs (lncRNAs) have important roles [6]. As ncRNAs, lncRNAs have the length of 200 nucleotides (nt) [7]. lncRNAs are identified as the crucial regulators involved in tumorigenesis [8]. lncRNAs function as tumor suppressors or oncogenes by either activating or suppressing the expression of protein-coding genes and hence participate in cell apoptosis, development, proliferation, invasion and migration [9]. Furthermore, most lncRNAs exhibit comparable roles in their potential to influence gene expression by various miRNAs, behavior connected with the competitive endogenous RNA (ceRNA) hypothesis [10].

Many lncRNAs influence the tumor cell cycle, cell proliferation, apoptosis, invasion, migration, and histone modifications. For example, the long-chain non-coding RNA SNHG1 upregulates MTDH through the various miR-145-5p, enhancing the viability, invasion, growth and migration of NSCLC [11]. lncRNA HULC promotes the tumorigenesis and metastasis of HCC by enhancing epithelial-mesenchymal transformation (EMT) by miR-200a-3p/ZEB1 pathway [12]. The FAM83A-AS1 is 1,572 nucleotides in length and transcribed based on FAM83A gene antisense strand in chromosome 8q24 [13]. FAM83A-AS1 has been implicated in the progression and development of non-small cell, hepatocellular, and esophageal malignancies [14–17].

Nonetheless, little is known about how FAM83A-AS1 enhances lung adenocarcinoma (LUAD).

microRNAs (miRNAs) are the endogenous RNAs showing a high evolutionary conservation degree, they are approximately 22 nucleotides in length and function to regulate gene levels post-transcriptionally by attaching to the target gene's 3' untranslated region (UTR) [18]. miRNAs exhibit a critical role in regulating several cancer-associated biological processes (BPs), such as cell growth, migration and apoptosis [19]. As a human miR-200 family (miR-200s) member, miR-141-3p is associated with the occurrence and development of many human cancers, including ovarian, bladder, and colorectal cancer (CRC) [20–22]. miR-141-3p level markedly decreased within LC cells and NSCLC tissues, and this downregulation predicted the dismal overall survival (OS) of NSCLC [23]. However, no interaction between hsa-miR-141-3p and lncRNA FAM83A-AS1 is detected within NSCLC.

This work focused on exploring the function of lncRNA FAM83A-AS1 in LUAD and its mechanism. The study revealed that FAM83A-AS1 was up-regulated, whereas miR-141-3p expression decreased within LUAD cells and tissues. As confirmed by further studies, inhibiting FAM83A-AS1 expression markedly promoted LUAD cell growth, invasion, migration and the EMT process. We hypothesized that FAM83A-AS1 functions in LUAD cells through targeting miR-141-3p; to test this hypothesis, we carried out rescue experiments. The goal of the current research was to identify a potentially viable target and biomarker for the therapeutic therapy and prognosis of LUAD.

2. Materials and Procedures

2.1. Moral proclamation

This research gained approval from Ethics Committee of the First Affiliated Hospital of Guangxi Medical University. Informed consents were obtained from patients prior to participating in any experimental activity with human tissues.

2.2 Bioinformatics analysis

The FAM83A-AS1 expression data in cancer tissues were obtained from LUAD patients and

normal subjects in the GEPIA and ENCORI databases and subjected to gene expression and survival analyses. The AnnoLnc2 database was used to reveal the miRNAs potentially bound to FAM83A-AS1 (33 miRNAs). The mirCode database was used to explore miRNAs (44 miRNAs) potentially bound to FAM83A-AS1. This study searched bindings sites of miR-141-3p and FAM83A-AS1 based on miRDB database. Data from the two databases was crossed to screen-out the target genes that might bind to FAM83A-AS1.

2.3. Clinical samples

Lung adenocarcinoma and neighboring normal tissues were obtained in pairs from 30 LUAD patients with pulmonary lobectomy at the Cardiothoracic Surgery Department of the Guangxi Medical University's First Affiliated Hospital from 2019 to 2020.

All tissue specimens were obtained from original malignant LUAD tumors and nearby normal tissues without any previous treatment and identified by the Department of Pathology. All fresh tissue samples were frozen immediately within liquid nitrogen prior to preservation under -80°C .

2.4. Cell culture

We obtained human LUAD H1299 cells and bronchial epithelial BEAS-2B cells from the Chinese Academy of Sciences (Shanghai). Wuhan Procell Life Technology Co., Ltd. provided the H1975 and A549 LUAD cell lines. This work cultivated the H1299 and BEAS-2B cells within DMEM (Gibco; Thermo). Meanwhile, H1975 cells were cultivated within RPMI-1640 medium (Gibco). All media included 1% penicillin/streptomycin (P1400; Solarbio) and 10% FBS (Gibco). We later cultivated cells within the humid incubator under 37°C and 5% CO_2 conditions. Later, we inoculated cells (1×10^6 /well) in 6-well plates, followed by transfection when the log-growth stage cells reached 80% confluence. The Guangzhou RiboBio Co., Ltd. developed and manufactured a small interfering RNA (siRNA) together with corresponding negative control (si-NC) for FAM83A-AS1. The sequences were as follows: si-FAM83A-AS1-1 is GCTGCCACCTACAAGA

TAA, si-FAM83A-AS1-2 is GGCCCTGGGCTGAATAATT, and si-FAM83A-AS1-3 is TGAGGCACAGTTTGAAAAA. This study acquired miR-141-3p inhibitor, miR-141-3p mimic, together with relevant NC (miR-141-3p NC) in Guangzhou RiboBio Co., Ltd. The A549, H1299, and H1975 cell lines were transfected using the Lipofectamine 3000 (L300015, Thermo). We harvested cells after they were transfected for 48 h, and evaluated the transfection rate through fluorescence-quantitative PCR (RT-qPCR).

2.5. RNA isolation and RT-qPCR

The RNA levels were detected through the RT-qPCR method. By adopting TRIzol reagent (Invitrogen), this study isolated total RNA from LUAD cells. Genomic DNA was removed for two min at 42°C using the reverse transcription kit (RR047A; Takara) and subsequently reverse transcribed for a 15-min period under 37°C . The RNA levels were detected through the RT-qPCR method. By adopting TRIzol reagent (Invitrogen), this study isolated total RNA from, followed by another 5-s under 85°C . We then conducted RT-qPCR with two μg of cDNA as the template, and PCR experiments were performed in the LightCycler480 System (Roche Ltd.) instrument. We performed the following thermal cycle, including 30-s under 95°C ; 5-s quantification under 95°C and 30-s under 60°C for altogether 40 cycles; 5-s melting under 95°C , 1-min under 60°C , and 1-cycle under 95°C ; 30-s cooling under 50°C . This work measured relative FAM83A-AS1, ZEB1, ZEB2, and microRNA expression using the $2^{-\Delta\Delta\text{Ct}}$ method. Internal benchmarks for normalization were GAPDH and U6. Sangon Biotech (Shanghai, China) was responsible for designing and synthesizing primers adopted in this work, followed by validation through BLAST analysis. Table 1 displays primers utilized in this work.

2.6. Dual-luciferase reporter assay

This study adopted miRDB to predict binding sites between miR-141-3p and FAM83A-AS1. The sequence of FAM83A-AS1 (wild-type-5'-CTCAACCAGCCCTTCAGTGTT-3', mutant-5'-GACATGGTCCCCTTGTACAA-3') was inserted into

Table 1. RT-qPCR primer sequences.

Primer		Sequence (5'–3')
FAM83A-AS1	Forward	CCCCAGAGCACTTCCTTAGC
	Reverse	CAGGGCCGTCTGTGTTACT
ZEB1	Forward	AGCAGTGAAAGAGAAGGGAATGC
	Reverse	GGTCCTCTCAGGTGCCTCAG
ZEB2	Forward	AGGCATATGGTGACGCACAA
	Reverse	CTTGAACCTGCGGTTACCTGC
hsa-miR-145-5p		GTCCAGTTTTCCAGGAATCCCT
hsa-miR-138-5p		AGCTGGTGTGTGAATCAGGCC
hsa-miR-489-3p		CCGTGACATCACATATACGGCAGC
hsa-miR-455-5p		CGCTATGTGCCTTTGGACTACATCG
hsa-miR-141-3p		TAACACTGTCTGGTAAAGATGG
hsa-miR-425-5p		AATGACACGATCACTCCCGTTGA
hsa-miR-383-5p		AGATCAGAAGGTGATTGTGGCT
hsa-miR-802		TGGCGCAGTAACAAAGATTATCCTTG
GAPDH	Forward	AGAAGGCTGGGGCTCATTTG
	Reverse	AGGGGCCATCCACAGTCTTC
U6	Forward	CTCGCTTCGGCAGCACAA
	Reverse	AACGCTTCACGAATTTGCGT

the pmiR-RB-ReportTM vector (Guangzhou RiboBio Co., Ltd.) to generate FAM83A-AS1-WT and FAM83A-AS1-MUT. Subsequently, we transfected the constructed reporter plasmid in cells exposed to miR-141-3p mimic-NC or miR-141-3p mimic transfection, respectively. At 48-h post-transfection, we adopted Dual-Glo[®] Luciferase Assay System (Promega) for determining luciferase activities under 37°C, and the firefly luciferase activity was standardized to the rennase activity.

2.7. Cell counting kit-8

After transfection with miR-141-3p inhibitor and si-FAM83A-AS1-1, we isolated or combined H1299 and A549 cells using CCK-8 reagent (C0037; Beyotime). Thereafter, cells (1×10^4 /mL) were inoculated in the 96-well plates. At the indicated 24, 48, and 72-h-time points, all wells were added with CCK-8 solution (10 μ L), followed by 4-h cell culture under 37°C. The microplate reader (Bio Rad Laboratories, Inc.) was adopted for determining cell absorbance (OD) value at 450 nm. Triplicate wells were set for each experimental condition, with their mean value as the level of cell proliferation under that condition.

2.8. EdU cell proliferation assay

The kits from the EdU Proliferation Assay (C0075S; Beyotime) were used and performed

according to the experimental procedures as recommended by the manufacturer. This work inoculated cells (5,000/well) into the 96-well plates and incubated for cell adherent growth. After 24 h of incubation, the EdU reaction solution at the concentration of 50 μ M was prepared with medium (100 μ L), and subsequently poured into each well of the 96-well plate. Thereafter, we incubated cells for a 2-h period under 37°C, followed by fixation using 4% paraformaldehyde (PFA) as well as Hoechst 33,342 (1:1000) staining. The inverted fluorescence difference microscope (Olympus, Tokyo, Japan) was employed to take cell photographs, while total and EdU-positive cells within the regions were counted.

2.9. Wound healing assay

After transfection, cells (3×10^5 /well) in the 6-well plates were inoculated for overnight incubation using serum-free medium under 37°C. When the cells had grown to about 90% confluence, we adopted the tip of a sterilized pipette tip (200- μ L) for gentle scratching at the 6-well plate center. After rinsing thrice with PBS, the cells from five regions of each group were imaged for 0 h by an optical microscope (Olympus). After 24 h, the migrated images were retaken in the same region by the microscope. The wound-healing zones were analyzed using the Image J software.

2.10. Transwell migration and invasion assay

Corning's 24-well 8.0-m transwell permeable supports was used for cell movement and invasion testing. This study coated Matrigel Matrix (BD Bioscience, USA) into the upper chamber and covered with the coating. Cell suspensions prepared at the concentration of 5×10^5 cells/mL were produced 24 h after cell transfection in the media without FBS. Then, we placed cell suspension (100 μ L) into the pre-coated Matrigel top chamber. Then, we poured 600 μ L of the medium that contained 10% FBS into the bottom transwell chamber for 24-h incubation. This work carefully wiped cells not penetrating matrix away using the cotton swab, followed by 4% PFA fixation on cells invading the lower chamber for 20 min. After fixation, cells were subject to 0.1% crystal violet

(Beyotime) staining. Later, cell number invading bottom chamber was determined, followed by counting using the optical microscope (Olympus) due to invasion. The same experimental protocol was performed for migration assays, except without covering the upper cavity membrane with Matrigel.

2.11. Western blotting (WB) assay

We isolated total cellular proteins in H1229 and A549 cells using RIPA buffer that contained protease inhibitor PMSF (Beyotime). Moreover, protein content was measured using BCA Protein Detection Kit (Beyotime). Total protein (40 μ g) and the pre-stained protein marker (5 μ L) (WJ103; EpiZyme) were analyzed through 8% SDS-PAGE, followed by transfer on PVDF membranes (P2438, SigmaAldrich, USA). Later, we blocked PVDF membranes using 5% skimmed milk under ambient temperature for a 1.5-h period, followed by overnight incubation using primary antibodies under 4°C. After being rinsed by TBST thrice, we further incubated PVDF membranes using HRP-labeled goat anti-rabbit IgG (PR30011, Proteintech) and goat antimouse IgG (PR30012, Proteintech) secondary antibodies under ambient temperature for a 1-h period. Finally, enhanced chemiluminescence (ECL, Beyotime) was performed to visualize protein bands on PVDF membranes and quantified with Image J software. The following primary antibodies were used: E-Cadherin (Cat. # 3195 T; 1:1000; Cell Signaling Technology, Inc (CST)), N-Cadherin (Cat. #: 13,116 T; 1:1000; CST), Vimentin (Cat. #: 5174 T; 1:1000; CST), ZEB1 (Cat. #: 3396 T; 1:1000; CST), ZEB2 (Cat. #: 97885S; 1:1000; CST). Normalization was performed with GAPDH.

2.12. Immunofluorescence (IF) assay

This study conducted the immunofluorescence assay for determining E-cadherin expression. In brief, cells were subject to 30-min 4% PFA fixation, incubation within 24-well plates, 20-min permeabilization using 0.5% TritonX-100, as well as 30-min blocking using 3% bovine serum albumin (BSA). We later incubated closed cells by primary antibody against E-cadherin (Cat. # 3195 T; 1:1000; CST) at 4°C overnight. Afterward, cells were incubated using goat anti-

rabbit IgG Alexa Fluor 488-tagged (H + L) (A0423) secondary antibody at 4°C for light avoidance for 60 min, and DAPI (C0065; Solarbio) was used to stain nuclei. Thereafter, the inverted fluorescence difference microscope (Olympus) was employed for obtaining photographs.

2.13. Statistical analysis

Each assay was carried out in triplicate. GraphPad Prism 7.0 and SPSS23.0 were also adopted for data analyses. The mean and standard deviation were used to represent the data. Two groups were compared by independent t-test, while LUAD and non-carcinoma tissues were compared by paired t-tests. Comparison among several groups was conducted by one-way ANOVA. $P < 0.05$ stood for statistical significance.

3. Results

We used functional assays for exploring FAM83A-AS1's effect on regulating the biological phenotype of LUAD cells. After predicting and validating miR-141-3p to be FAM83A-AS1's downstream target, different rescue assays were performed for determining whether lncRNA FAM83A-AS1's tumor-promoting function is dependent on its regulation of miR-141-3p. According to our findings, FAM83A-AS1 enhanced LUAD cell EMT, growth, invasion and migration through targeting miR-141-3p. Our results add to our understanding of the pathogenesis and therapy of lung cancer.

3.1 LncRNA FAM83A-AS1 level increased within LUAD samples, which predicted poor patient prognosis

The GEPIA and ENCORI databases were collected to acquire data on FAM83A-AS1 expression within tumor samples. As a result, FAM83A-AS1 level was anomalous in several malignancies compared with normal tissues and significantly upregulated in LUAD tissues (Figure 1a). According to Kaplan-Meier (K-M) analysis results, FAM83A-AS1 down-regulated was related to improved patient outcomes (Figure 1b). To corroborate these findings, we employed RT-qPCR assays to determine FAM83A-AS1 levels within LUAD as well as corresponding

tissues from 30 LUAD patients (Figure 1c). Correlation of FAM83A-AS1 level with clinicopathological factors among LUAD cases was analyzed, which indicated the relation of FAM83A-AS1 level with tumor size and histological differentiation in LUAD patients (Table 2). Furthermore, FAM83A-AS1 mRNA levels were consistently greater within LUAD cells (A549, H1299, H1975) compared with healthy BEAS-2B cells. (Figure 1d). Because FAM83A-AS1 expression was greater within H1299 and A549 cells, they were selected for subsequent analyses. The data suggest that the lncRNA FAM83A-AS1 is likely to be substantially linked to the development of LUAD and that FAM83A-AS1 may be an effective tumor marker for LUAD.

3.2 Silencing of FAM83A-AS1 decreases proliferation, migration, and invasion in LUAD cells, as well as EMT processes

To validate FAM83A-AS1's contribution to the growth of LUAD cells, we transfected siRNA

against FAM83A-AS1 in H1299 and A549 cells. Relative to controls, si-FAM83A-AS1-1 silenced the best in both sets of cell lines (Figure 2a). Hence we chose si-FAM83A-AS1-1 sequence for the subsequent experiments. Meanwhile, we conducted EdU and CCK8 assays for confirming FAM83A-AS1's role in H1299 and A549 cell growth. The CCK8 and EdU techniques were used for verifying FAM83A-AS1's role in H1299 and A549 cells. We observed silencing FAM83A-AS1 with siRNA significantly reduced cell growth (Figure 2b-c). Wound healing investigations and Transwell assays, consistently validated FAM83A-AS1's effect on A549 and H1299, specifically that silencing FAM83A-AS1 inhibited cell migration and invasion (Figure 2d-e). Protein blotting evaluated the amounts of proteins related to EMT in LUAD cells. Inhibiting FAM83A-AS1 greatly boosted the protein levels of E-cadherin, a critical epithelial marker, whereas decreasing the expression of the critical mesenchymal marker genes Vimentin and N-cadherin within H1299

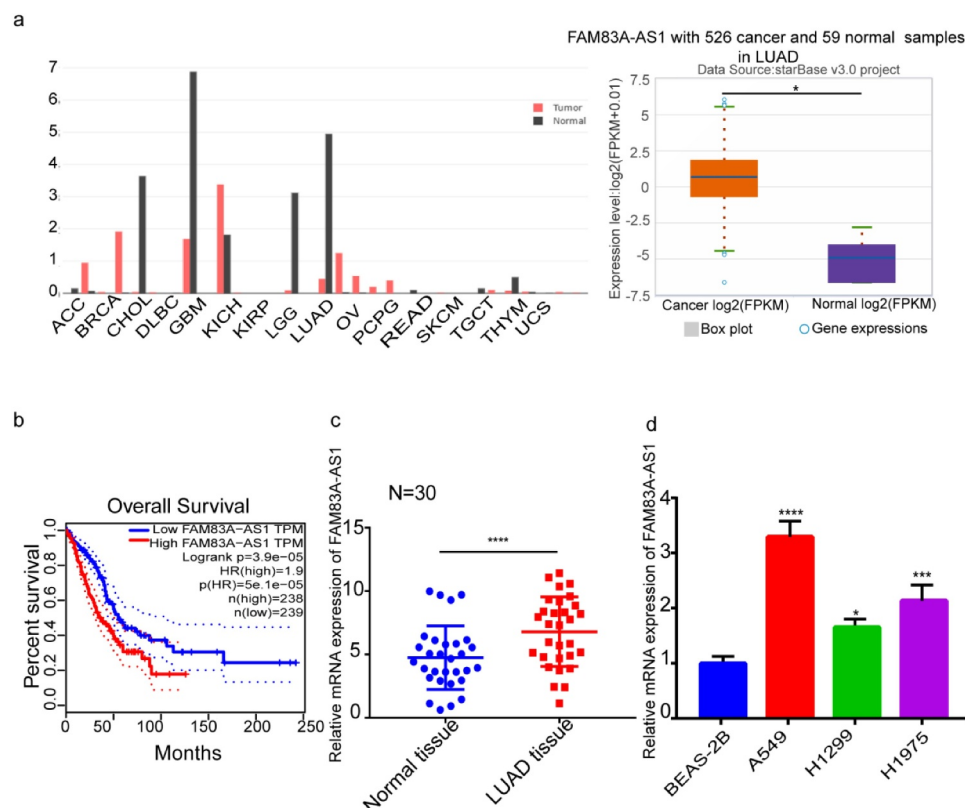


Figure 1. LncRNA FAM83A-AS1 expression increased within LUAD samples, which predicts dismal patient survival. (a) The GEPIA and ENCORI databases demonstrated that the FAM83A-AS1 level was aberrant within several tumor samples, and the expression within LUAD tissues increased compared with healthy tissue samples. (b) LUAD cases showing higher FAM83A-AS1 levels had dismal OS, according to the GEPIA website. (c) RT-qPCR was used for detecting the FAM83A-AS1 expression levels in the cancerous and adjacent tissues of LUAD in 30 patients. (d) As suggested by qRT-PCR analysis, FAM83A-AS1 mRNA levels were consistently higher in the LUAD cell lines (A549, H1299, and H1975) than in healthy BEAS-2B cells. * $P < 0.05$, ** $P < 0.01$, *** $P < 0.001$.

Table 2. Association of FAM83A-AS1 expression with clinicopathological parameters from patients.

Variable	n	FAM83A-AS1 expression		P value
		Low	High	
Total	30	10	20	
Gender				
Male	19	6	13	0.548
Female	11	4	7	
Age(years)				
<60	18	4	14	0.139
≥60	12	6	6	
Tumor size(cm)				
≤3	16	2	14	0.019
>3	13	8	6	
History of smoking				
No	17	5	12	0.705
Yes	13	5	8	
Differentiation				
Well	8	2	6	0.682
Poor+Moderate	22	8	14	
Lymph node metastasis				
No	10	6	4	0.045
Yes	20	4	16	
TNM stage				
I-II	21	4	17	0.3
III-IV	9	6	3	

and A549 cells. These data offer evidence that silencing FAM83A-AS1 inhibits the EMT, growth, invasion and migration of LUAD cells.

3.3 MiR-141-3p is FAM83A-AS1's potential target, which shows negative relation to FAM83A-AS1

Two databases were used to search for FAM83A-AS1 target genes (StarBase and AnnoLnc2). Figure 3a depicts the miRNAs that were predicted jointly in both databases. We conducted RT-qPCR for investigating the relation of such miRNAs with FAM83A-AS1. Suppressing FAM83A-AS1 had no effect on miR-489-3p or miR-455-5p expression, but had a significant effect on miR-138-5p, miR-425-5p, miR-141-3p, miR-145-5p, miR-802, and miR-383-5p expression, with the most pronounced effect on miR-141-3p (Figure 3b). Following that, miR-141-3p expression decreased within LUAD tissue samples, as revealed by RT-qPCR; besides, miR-141-3p levels within H1299 and A549 cells markedly decreased within BEAS-2B cells (Figure 3c). This study also performed RT-qPCR for assessing miR-141-3p mimics and inhibitors' transfection efficiency (Figure 3d). To this end, we verified the association of FAM83A-AS1 with miR-141-3p by luciferase reporter assays. The results indicated that, cells subject

to co-transfection of miR-141-3p mimic with FAM83A-AS1-WT had considerably lower luciferase activity than those subject to co-transfection of mimic NC with FAM83A-AS1-WT. Nonetheless, co-transfection with FAM83A-AS1-MUT and miR-141-3p mimic did not markedly change luciferase activity, which suggested the binding relation between miR-141-3p and 3'UTR of FAM83A-AS1 (Figure 3e). These data point to FAM83A-AS1 promoting LUAD cell growth via miR-141-3p regulation.

3.4 The inhibitor of miR-141-3p restored FAM83A-AS1 silencing' inhibition on LUAD cell EMT, growth, migration and invasion

To further investigate whether FAM83A-AS1 regulated miR-141-3p within LUAD cells, we transfected the miR-141-3p inhibitor into the cells, which silenced miR-141-3p. After the co-transfection of si-FAM83A-AS1-1 with miR-141-3p inhibitor, A549 and H1299 cells proliferated faster than when si-FAM83A-AS1-1 has transfected alone (Figure 4a); The effect of FAM83A-141-3p silencing was reversed by FAM83A-AS1-1 knockdown's suppression on H1299 and A549 cell invasion and migration by 141-3 p inhibitor (Figure 4b). Similarly, when miR-141-3p inhibitor was co-transfected with si-FAM83A-AS1-1, EMT-related protein levels, including N-cadherin, Vimentin, and E-cadherin exhibited opposite trends in si-FAM83A-AS1-1+ miR-141-3p inhibitors compared with cells with si-FAM83A-AS1-1 + inhibitor NC (Figure 4c). FAM83A-AS1-1 knockdown resulted in elevated E-cadherin levels in lung cancer cells, but E-cadherin levels could be suppressed by miR-141-3p inhibitor exposure (Figure 4d). Our data suggest that inhibiting miR-141-3p suppresses FAM83A-AS1 knockdown's suppression on EMT, growth, migration and invasion of LUAD cells.

3.5 ZEB1 and ZEB2 may be FAM83A-AS1 and miR-141-3p target genes

Tumor cell invasion and metastases rely on EMT. We predicted miR-141-3p's target against TargetScan for investigating its downstream targets. Research has demonstrated the target of miR-141-3p in colorectal, breast, and lung cancer and that ZEB1 and ZEB2 expression is implicated in EMT processes; thus, we picked ZEB1 and ZEB2. MiR-141-

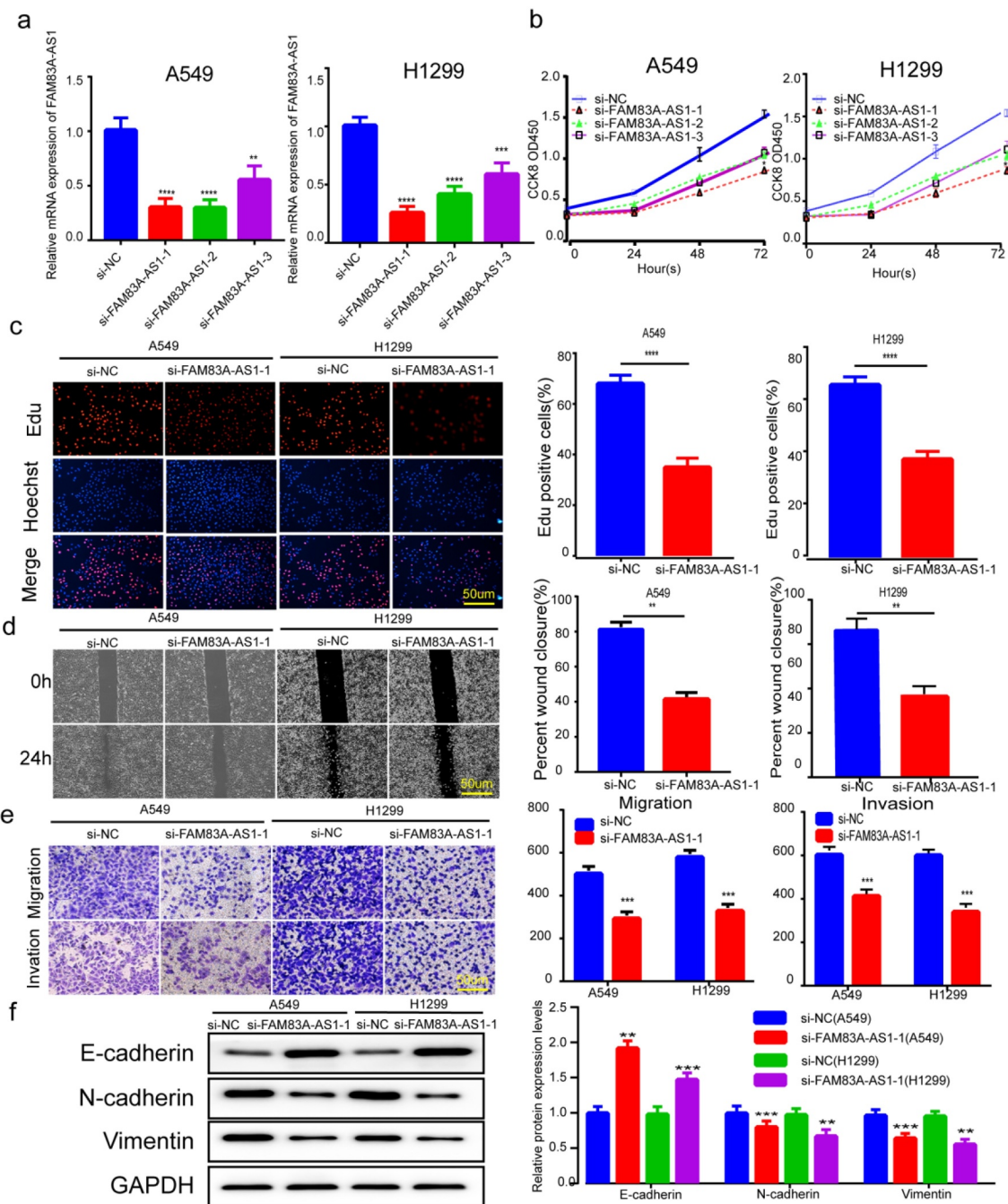


Figure 2. FAM83A-AS1 silencing-inhibited LUAD cell EMT, growth, invasion and migration. (a) Three siRNAs were transfected into H1299 and A549 cells, then qRT-PCR was performed for determining FAM83A-AS1 mRNA expression. (b-c) EdU and CCK8 assays were performed to detect LUAD cell proliferation. (d-e) Transwell and scratch assays were performed to examine the effect of silencing of FAM83A-AS1 on H1299 and A549 cells. (f) EMT-related protein levels were measured through WB assay. * $P < 0.05$, ** $P < 0.01$, *** $P < 0.001$.

3p's commonly acknowledged targeted oncogenes within tumors are ZEB1 and ZEB2. In various cancers, the TCGA database revealed a negative connection of miR-141-3p with ZEB1 level. Likewise, ZEB2 and miR-141-3p expression levels were inversely associated with several cancers (Figure 5a). After

FAM83A-AS1 suppression, ZEB1 and ZEB2 were less expressed, but mRNA levels of ZEB1/ZEB2 mRNA expression was abolished when H1299 and A549 cells were co-transfected using miR-141-3p inhibitors (Figure 5b). Protein blotting tests revealed that following FAM83A-AS1 silencing, ZEB1/ZEB2

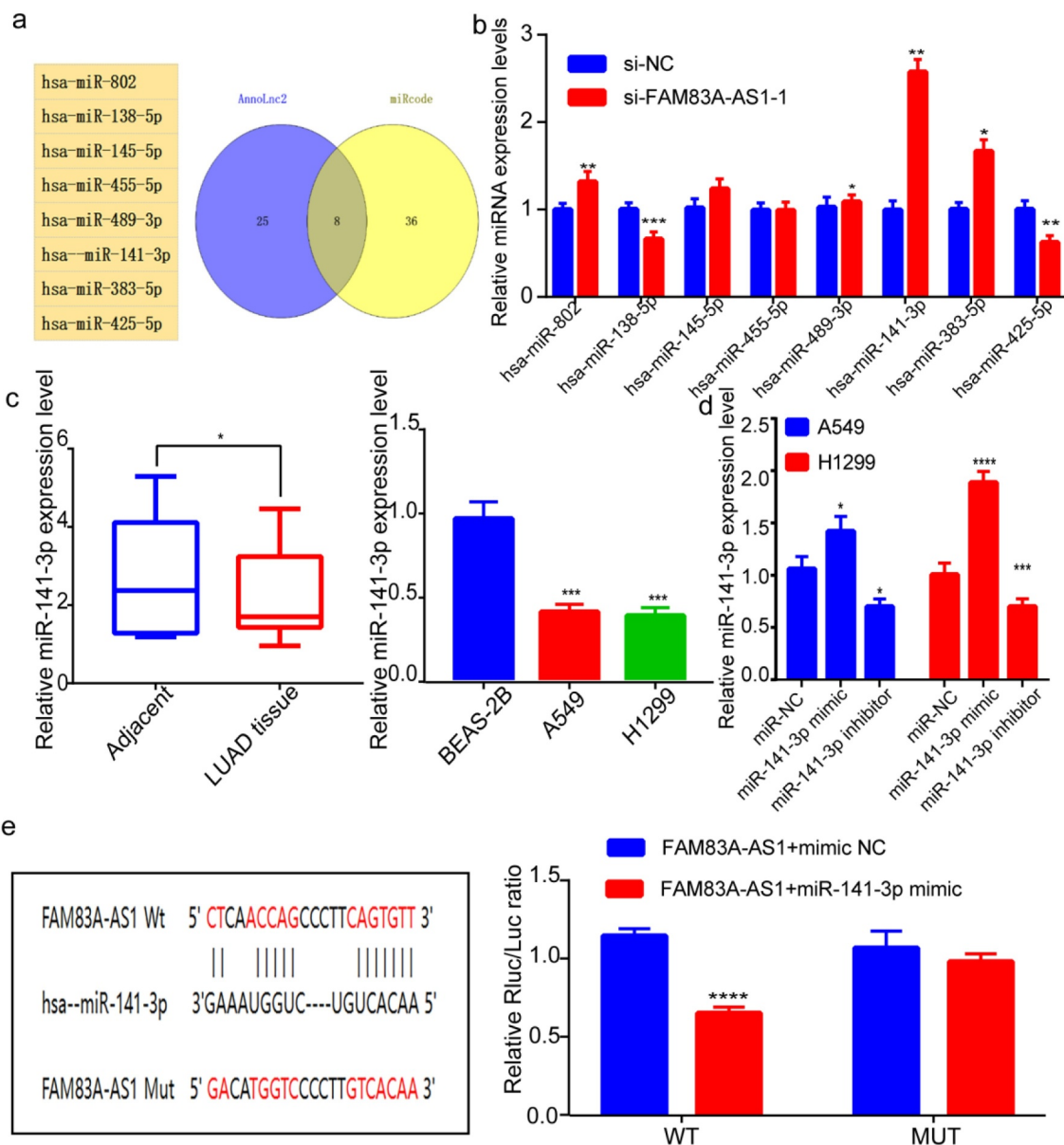


Figure 3. MiR-141-3p is FAM83A-AS1's target, which shows negative relation to FAM83A-AS1 (a) Targeted miRNAs of FAM83A-AS1 as jointly predicted by the StarBase and AnnoLnc2 database; (b) RT-qPCR was conducted to determine the targeted relationship between miRNAs and FAM83A-AS1. (c) miR-141-3p levels within A549, BEAS-2B and H1299 cell lines and tissues; (d) RT-qPCR was performed to measure miR-141-3p inhibitors/mimics' transfection efficiency; (e) Pre-predicted miR-141-3p's binding site within FAM83A-AS1, dual-luciferase reporter assay was conducted to analyze the interaction of FAM83A-AS1 with miR-141-3p. * $P < 0.05$, ** $P < 0.01$, *** $P < 0.001$.

protein expression decreased, and that in miR-141-3p mimics group decreased relative to NC group (Figure 5c). To see if FAM83A-AS1's effect on regulating ZEB1/ZEB2 was determined by miR-141-3p, this work co-transfected cells with miR-141-3p inhibitors and si-FAM83A-AS1, and the regulatory effect of FAM83A-AS1 on ZEB1 and ZEB2 expression was reversed (Figure 5d). According to the findings,

FAM83A-AS1 modulates ZEB1/ZEB2 levels via the sponge of miR-141-3p.

4 Discussion

The present work found the up-regulation of FAM83A-AS1 within LUAD, while miR-141-3p showed minimal expression and that inhibiting

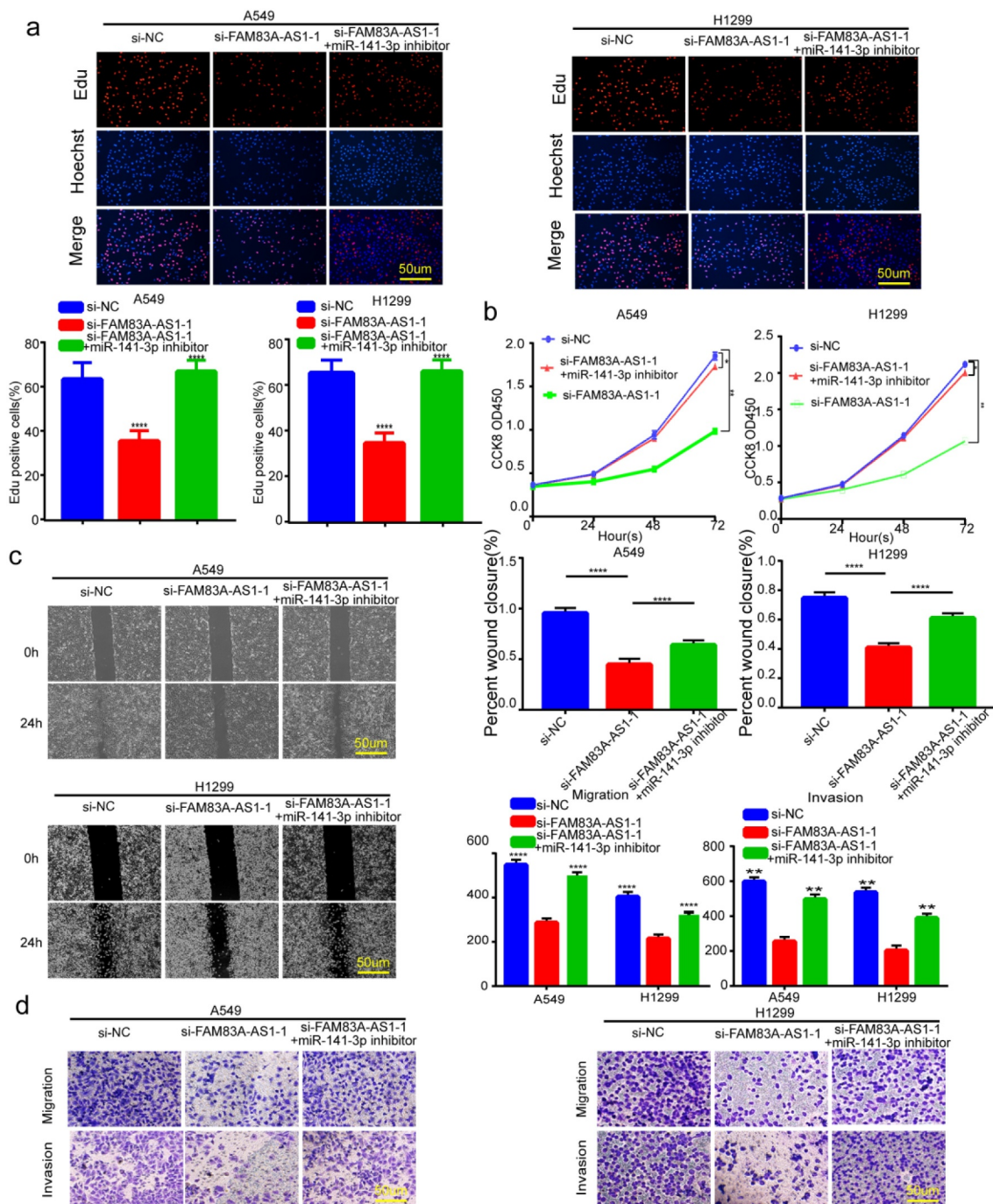


Figure 4. miR-141-3p inhibitor abolished FAM83A-AS1 silencing's suppression on LUAD cell EMT, growth, migration and invasion. (a-b) H1299 and A549 cell proliferation measured through Edu and CCK8 assays; (c-d) Scratch and Transwell assays conducted to examine H1299 and A549 cell invasion and migration; (e) EMT-related protein levels within H1299 and A549 cells through WB assay; (f) E-cadherin protein levels were determined in A549 and H1299 by immunofluorescence.

FAM83A-AS1 increases miR-141-3p expression. Furthermore, downregulation of FAM83A-AS1 resulted in an elevated expression of miR-141-3p, which greatly blocked EMT, invasion and migration of LUAD cells. According to our findings, the

FAM83A-AS1/miR-141-3p axis seems crucial in LUAD formation and progression.

One of the fundamental methods by which lncRNA modulates gene expression is its interaction with miRNA as a ceRNA and binding to

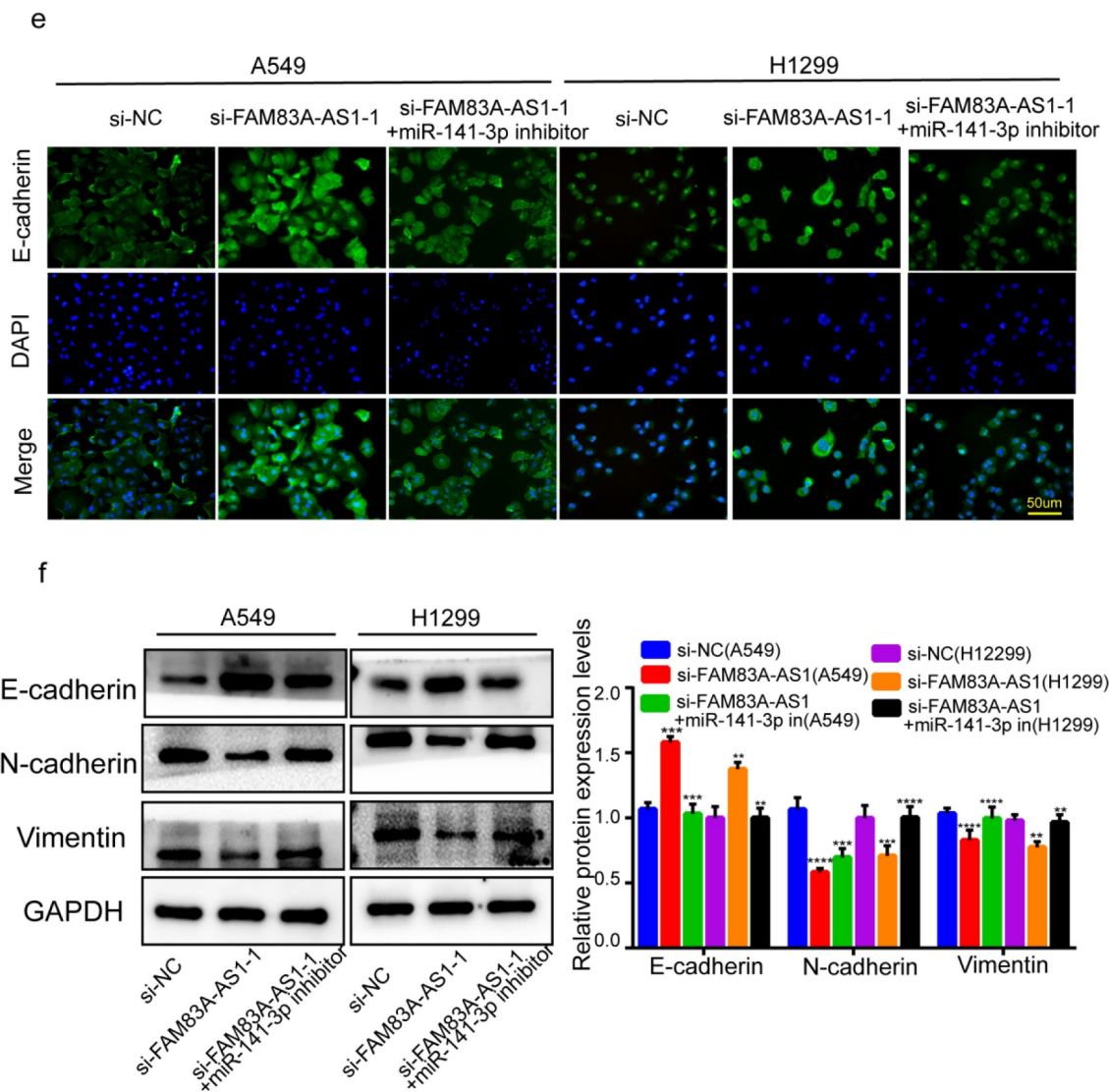


Figure 4. Continue

miRNA response elements to defend miRNA from binding to the target RNA [24]. LncRNAs play a vital role in lncRNAs as ceRNAs mediate miRNAs in various cellular processes. For example, lncRNA ACTA2-AS1 upregulates SMAD3 by functioning as a ceRNA of miR-143-3p, encouraging cervical cancer development [25]. Linc00673 acts as a miR-150-5p sponge that regulates the expression of the E-cadherin, affecting NSCLC31 proliferation, migration, invasion, and EMT [26].

Cancer metastasis accounts for a major cause leading to cancer-associated mortality, which leads to about 90% of cancer-related deaths, while EMT

has an important effect on this [27]. EMT is intercellular adhesion and epithelial cell polarity loss, together with the development of mesenchymal-like characteristics and enhanced motility [28]. During the development of the spindle cell invasive phenotype, epithelial marker proteins (E-cadherin) were progressively lost, whereas mesenchymal markers like vimentin and N-cadherin were relatively more abundant [29,30]. Reduced E-cadherin expression is a prominent feature of EMT and is a vital element in cancer metastasis. The transcription factors Snail1, Snail2, ZEB-1 and Twist regulate E-cadherin transcription [28,31]. A report discovered that miR-200 family members could inhibit

EMT by targeting E-cadherin to inhibit the transcription factors ZEB1 and ZEB2 [32].

MiR-141-3p is the tumor suppressor [33]. miR-141-3p levels markedly decrease within NSCLC cells and tissues, which predict the dismal overall survival (OS) of NSCLC cases [23]. Besides, miR-141-3p is suggested to enhance NSCLC cell growth via modulating PHLPP1 and PHLPP2 [34]. MiRNAs have been extensively related to EMT, which modulate EMT-related protein levels [33].

MiR-182-5p, for example, influences EMT through decreasing E-cadherin, vimentin, N-cadherin, ZEB2 and snail proteins, while NSCLC suppresses metastasis and invasion [35].

Our investigation demonstrated that knocking down FAM83A-AS1 significantly inhibited EMT in lung cancer cells. We conducted additional research to confirm the molecular mechanism FAM83A-AS1 targets miR-141-3p to control EMT. We revealed that FAM83A-AS1 can target

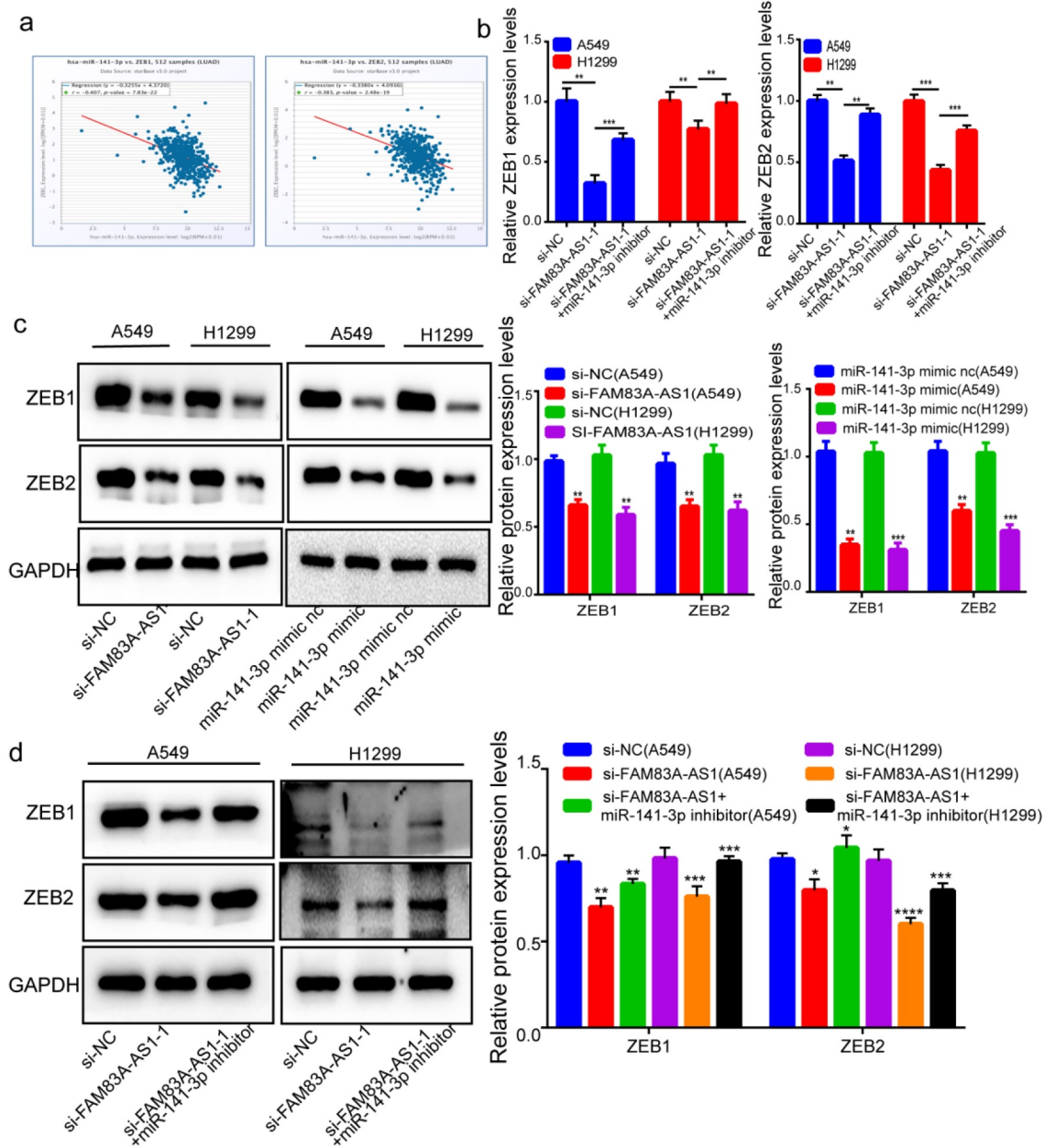


Figure 5. Both ZEB1 and ZEB2 recognized as miR-141-3p and FAM83A-AS1' target genes. (a) The TCGA database indicated a negative correlation trend between miR-141-3p and ZEB1 and ZEB2; (b) relative expression of ZEB1 and ZEB2 in LUAD cells determined through RT-qPCR; (c-d) ZEB1/ZEB2 protein levels determined by Western blotting.

miR-141-3p to alter EMT-associated protein levels. According to the chemical structure, StarBaseV2.0 suggests that FAM83A-AS1 may have miR-141-3p's binding site. Double luciferase studies confirmed our assumptions about the link between FAM83A-AS1 and miR-141-3p. Our findings illustrated that miR-141-3p has an inverse relationship with FAM83A-AS1 and that miR-141-3p reverses FAM83A-AS1's effect on LUAD cells. Our experiments also confirmed a regulatory relation of miR-141-3p with ZEB1/ZEB2, which, when combined with Studies [22] with dual-luciferase experiments, suggested the role of miR-141-3p in the epithelial-mesenchymal transformation process of NSCLC by directly targeting the binding of the 3'UTR sequences of ZEB2 and ZEB1. These findings imply that FAM83A-AS1 may operate as the miR-141-3p sponge, which promotes EMT-related molecule expression, including ZEB1 and ZEB2.

5 Conclusion

The findings of this work define the roles and mechanisms through which FAM83A-AS1 promotes EMT and EMT-related molecules to regulate LUAD metastasis via miR-141-3p targeting. These findings imply that FAM83A-AS1 is a significant target for predicting patient survival, which is the potential anti-LC therapeutic target. This experiment, however, lacks crucial therapeutically relevant findings, such as the link between FAM83A-AS1 and miR-141-3p and patient clinical prognostic data. This work did not evaluate the binding link of miR-141-3p with ZEB1/ZEB2 by dual-luciferase assays, but further experiments can elucidate it. Furthermore, comprehensive experimental analyses will be required to decipher the individual signaling pathways and signaling proteins regulated by FAM83A-AS1 and hsa-miR-141-3p.

Highlights

- FAM83A-AS1 expression markedly increased within LUAD.

- Silencing of FAM83A-AS1 reduces the LUAD cell EMT, proliferation, invasion and migration.
- miR-141-3p was identified as a FAM83A-AS1 sponge.
- ZEB1 and ZEB2 were identified as miR-141-3p targets.

Notes

Conceived and designed the experiments: Hongyu Huang, Yanbin Wu, Qichen Zhang

Performed the experiments: Hongyu Huang, Chuyi Yang, Ting Zhuo

Statistical analysis: Xiaohong Li, Nijiao Li, Jinyan Gan

Wrote the paper: Hongyu Huang, Lu Zhu, Chenyang Luo

All authors read and approved the final manuscript.

Disclosure statement

No potential conflict of interest was reported by the author(s).

Funding

This work was supported by the Scientific research project funded by the Guangxi Health Commission [grant no. Z20180975]; Guangxi Appropriate Medical and Health Care Technology Promotion Project [grant no. S2020026].

References

- [1] Siegel RL, Miller KD, Fuchs HE, et al. Cancer statistics, 2021. *CA Cancer J Clin.* 2021;71(1):7–33.
- [2] Chen W, Zheng R, Baade PD, et al. Cancer statistics in China, 2015. *CA Cancer J Clin.* 2016;66(2):115–132.
- [3] Zhang C, Zhang Z, Zhang G, et al. Clinical significance and inflammatory landscapes of a novel recurrence-associated immune signature in early-stage lung adenocarcinoma. *Cancer Lett.* 2020;479:31–41.
- [4] Wang H, Kanmangne D, Li R, et al. miR-30a-3p suppresses the proliferation and migration of lung adenocarcinoma cells by downregulating CNPY2. *Oncol Rep.* 2020;43(2):646–654.
- [5] Wood SL, Pernemalm M, Crosbie PA, et al. Molecular histology of lung cancer: from targets to treatments. *Cancer Treat Rev.* 2015;41(4):361–375.
- [6] Mattick JS. Non-coding RNAs: the architects of eukaryotic complexity. *EMBO Rep.* 2001;2(11):986–991.
- [7] St Laurent G, Wahlestedt C, Kapranov P. The Landscape of long noncoding RNA classification. *Trends Genet.* 2015;31(5):239–251.

- [8] Lin C, Yang L. Long noncoding RNA in cancer: wiring signaling circuitry. *Trends Cell Biol.* 2018;28(4):287–301.
- [9] Wei S, Du M, Jiang Z, et al. Long noncoding RNAs in regulating adipogenesis: new RNAs shed lights on obesity. *Cell Mol Life Sci.* 2016;73(10):2079–2087.
- [10] Li DS, Ainiwaer JL, Sheyhiding I, et al. Identification of key long non-coding RNAs as competing endogenous RNAs for miRNA-mRNA in lung adenocarcinoma. *Eur Rev Med Pharmacol Sci.* 2016;20(11):2285–2295.
- [11] Lu Q, Shan S, Li Y, et al. Long noncoding RNA SNHG1 promotes non-small cell lung cancer progression by up-regulating MTDH via sponging miR-145-5p. *FASEB J.* 2018;32(7):3957–3967.
- [12] Li SP, Xu HX, Yu Y, et al. LncRNA HULC enhances epithelial-mesenchymal transition to promote tumorigenesis and metastasis of hepatocellular carcinoma via the miR-200a-3p/ZEB1 signaling pathway. *Oncotarget.* 2016;7(27):42431–42446.
- [13] Parameswaran N, Bartel CA, Hernandez-Sanchez W, et al. A FAM83A positive feed-back loop drives survival and tumorigenicity of pancreatic ductal adenocarcinomas. *Sci Rep.* 2019;9(1):13396.
- [14] Huang GM, Zang HL, Geng YX, et al. LncRNA FAM83A-AS1 aggravates the malignant development of esophageal cancer by binding to miR-495-3p. *Eur Rev Med Pharmacol Sci.* 2020;24(18):9408–9415.
- [15] Xiao G, Wang P, Zheng X, et al. FAM83A-AS1 promotes lung adenocarcinoma cell migration and invasion by targeting miR-150-5p and modifying MMP14. *Cell Cycle.* 2019;18(21):2972–2985.
- [16] Jia J, Li H, Chu J, et al. LncRNA FAM83A-AS1 promotes ESCC progression by regulating miR-214/CDC25B axis. *J Cancer.* 2021;12(4):1200–1211.
- [17] Wang W, Zhao Z, Xu C, et al. LncRNA FAM83A-AS1 promotes lung adenocarcinoma progression by enhancing the pre-mRNA stability of FAM83A. *Thorac Cancer.* 2021;12(10):1495–1502.
- [18] Cho HJ, Liu G, Jin SM, et al. MicroRNA-205 regulates the expression of Parkinson's disease-related leucine-rich repeat kinase 2 protein. *Hum Mol Genet.* 2013;22(3):608–620.
- [19] Bartel DP. MicroRNAs: genomics, biogenesis, mechanism, and function. *Cell.* 2004;116(2):281–297.
- [20] Masoumi-Dehghi S, Babashah S, Sadeghizadeh M. microRNA-141-3p-containing small extracellular vesicles derived from epithelial ovarian cancer cells promote endothelial cell angiogenesis through activating the JAK/STAT3 and NF- κ B signaling pathways. *J Cell Commun Signal.* 2020;14(2):233–244.
- [21] Yang X, Wang P. MiR-188-5p and MiR-141-3p influence prognosis of bladder cancer and promote bladder cancer synergistically. *Pathol Res Pract.* 2019;215(11):152598.
- [22] Liu X, Wang C. Long non-coding RNA ATB is associated with metastases and promotes cell invasion in colorectal cancer via sponging miR-141-3p. *Exp Ther Med.* 2020;20(6):261.
- [23] Li W, Cui Y, Wang D, et al. MiR-141-3p functions as a tumor suppressor through directly targeting ZFR in non-small cell lung cancer. *Biochem Biophys Res Commun.* 2019;509(3):647–656.
- [24] Cao C, Zhang T, Zhang D, et al. The long non-coding RNA, SNHG6-003, functions as a competing endogenous RNA to promote the progression of hepatocellular carcinoma. *Oncogene.* 2017;36(8):1112–1122.
- [25] Luo L, Wang M, Li X, et al. A novel mechanism by which ACTA2-AS1 promotes cervical cancer progression: acting as a ceRNA of miR-143-3p to regulate SMAD3 expression. *Cancer Cell Int.* 2020;20:372.
- [26] Lu W, Zhang H, Niu Y, et al. Erratum to: long non-coding RNA linc00673 regulated non-small cell lung cancer proliferation, migration, invasion and epithelial mesenchymal transition by sponging miR-150-5p. *Mol Cancer.* 2017;16(1):144.
- [27] Valastyan S, Weinberg RA. Tumor metastasis: molecular insights and evolving paradigms. *Cell.* 2011;147(2):275–292.
- [28] Ahmed RA, Alawin OA, Sylvester PW. γ -Tocotrienol reversal of epithelial-to-mesenchymal transition in human breast cancer cells is associated with inhibition of canonical Wnt signalling. *Cell Prolif.* 2016;49(4):460–470.
- [29] Bakiri L, Macho-Maschler S, Custic I, et al. Fra-1/AP-1 induces EMT in mammary epithelial cells by modulating Zeb1/2 and TGF β expression. *Cell Death Differ.* 2015;22(2):336–350.
- [30] Suh Y, Yoon CH, Kim RK, et al. Claudin-1 induces epithelial-mesenchymal transition through activation of the c-Abl-ERK signaling pathway in human liver cells. *Oncogene.* 2013;32(41):4873–4882.
- [31] Serrano-Gomez SJ, Maziveyi M, Alahari SK. Regulation of epithelial-mesenchymal transition through epigenetic and post-translational modifications. *Mol Cancer.* 2016;15:18.
- [32] Zhou X, Wang Y, Shan B, et al. The downregulation of miR-200c/141 promotes ZEB1/2 expression and gastric cancer progression. *Med Oncol.* 2015;32(1):428.
- [33] Langer EM, Kendsersky ND, Daniel CJ, et al. ZEB1-repressed microRNAs inhibit autocrine signaling that promotes vascular mimicry of breast cancer cells. *Oncogene.* 2018;37(8):1005–1019.
- [34] Mei Z, He Y, Feng J, et al. MicroRNA-141 promotes the proliferation of non-small cell lung cancer cells by regulating expression of PHLPP1 and PHLPP2. *FEBS Lett.* 2014;588(17):3055–3061.
- [35] Sun Y, Fang R, Li C, et al. Hsa-mir-182 suppresses lung tumorigenesis through down regulation of RGS17 expression in vitro. *Biochem Biophys Res Commun.* 2010;396(2):501–507.